

Dual Degradation-Inspired Deep Unfolding Network for Low-Light Image Enhancement

Huake Wang, Xingsong Hou *Member, IEEE*, Xiaoyang Yan

Abstract—Although low-light image enhancement has achieved great stride based on deep enhancement models, most of them mainly stress on enhancement performance via an elaborated black-box network and rarely explore the physical significance of enhancement models. Towards this issue, we propose a Dual degradAdation-inSpired deep Unfolding network, termed DASUNet, for low-light image enhancement. Specifically, we construct a dual degradation model (DDM) to explicitly simulate the deterioration mechanism of low-light images. It learns two distinct image priors via considering degradation specificity between luminance and chrominance spaces. To make the proposed scheme tractable, we design an alternating optimization solution to solve the proposed DDM. Further, the designed solution is unfolded into a specified deep network, imitating the iteration updating rules, to form DASUNet. Local and long-range information are obtained by prior modeling module (PMM), inheriting the advantages of convolution and Transformer, to enhance the representation capability of dual degradation priors. Additionally, a space aggregation module (SAM) is presented to boost the interaction of two degradation models. Extensive experiments on multiple popular low-light image datasets validate the effectiveness of DASUNet compared to canonical state-of-the-art low-light image enhancement methods. Our source code and pretrained model will be publicly available.

Index Terms—Low-light image enhancement, dual degradation model, deep unfolding network, alternating optimization, space aggregation module.

I. INTRODUCTION

DUE to lacking of suitable light source, images shot at the surrounding exhibit poor visibility, weak contrast, and unpleasant noise. It not only prejudices the visual comfort of the observer, but also impairs the analysis performance of down-stream high-level vision tasks, e.g., detection [1]–[4], tracking [5], [6], recognition [7], [8], and segmentation [9]–[11]. Hence, how to restore low-light images is an urgent problem to be solved.

Low-light image enhancement refers to improving the brilliance of image content and rendering the radiance of image focus. Generally, an image is considered as the product of an luminance layer and a reflectance layer based on Retinex theory [12]. Mathematically, it can be defined as $I = L \otimes R$, where \otimes denotes the element-level multiplication, L and R are the luminance layer and the reflectance layer which imply the

extrinsic brightness and the intrinsic property of an object, respectively. According to the statement, some traditional methods attempt to separate reflectance maps from low-light images as enhanced results via Gaussian filter [12], multi-scale Gaussian filter [13], or luminance structure prior [14]. However, they could produce some unnatural appearances. Alternatively, some researchers simultaneously increase luminance component and restore reflectance component to further adjust under-exposure images via bright-pass filter [15] and weighted variational model [16]. Unfortunately, this way could under-enhance or over-enhance these images with uneven brightness. Besides, several additional penalty constraints, e.g., noise prior [17], low-rank constraint [18], structure prior [19], [20], are combined into the final optimization objective function to further improve the image objective quality. However, hand-crafted priors could not well encapsulate the various real low-light scenes. In short, above traditional methods are hard to yield impressive enhancement performance.

Fueled by convolutional neural network, a large group of researchers have attempted to train high-efficient low-light image enhancement models from a sea of data. Deep black-box methods directly learn a powerful mapping relationship from low-light images to normal-light images via denoising autoencoder [21], multi-scale framework [22]–[25], normalizing flow [26], transformer [27], [28], deep unsupervised framework [29], [30], and so on. However, they focus more on enhancement performance at the expense of the interpretability and physical degradation principle, which could heavily hinder the performance improvements. In the light of imaging theory, Retinex-based deep models are proposed to decompose natural images to luminance layers and reflectance layers, which could be trained via reflectance layer consistency constraint [31], [32], luminance smoothness [33], semantic-aware prior [34], and reference-free architecture search [35]. However, above methods only mimic ill-posed decomposition in form but lack accurate luminance references. Moreover, URetinex [36] unrolled Retinex theory into a convolutional network to combine the physical principle and powerful learning ability of deep model from tremendous natural images. But it was imposed with too many constraints and cannot learn an efficient and robust enhancement model.

To address the aforementioned issues, we propose a Dual degradAdation-inSpired deep Unfolding network, termed **DASUNet**, for low-light image enhancement, which is shown in Figure 1. The motivation originates from the degradation specificity of low-light images between luminance and chrominance spaces [37]–[39]. On this basis, we formulate the task of low-light image enhancement as the optimization

Manuscript received August -, 2021; revised -, 2022. This work was supported in part by the NSFC of China under Grant (61872286; 62272376), Key R&D Program of Shaanxi Province of China under Grant (2020ZDLGY04-05; S2021-YF-YBSF-0094). (Corresponding author: Xingsong Hou.)

Huake Wang, Xingsong Hou, and Xiaoyang Yan are with the School of Information and Communications Engineering, Xi'an Jiaotong University, Xi'an 710049, China (e-mail: wanghuake@stu.xjtu.edu.cn; houxs@mail.xjtu.edu.cn; xyyan@stu.xjtu.edu.cn).

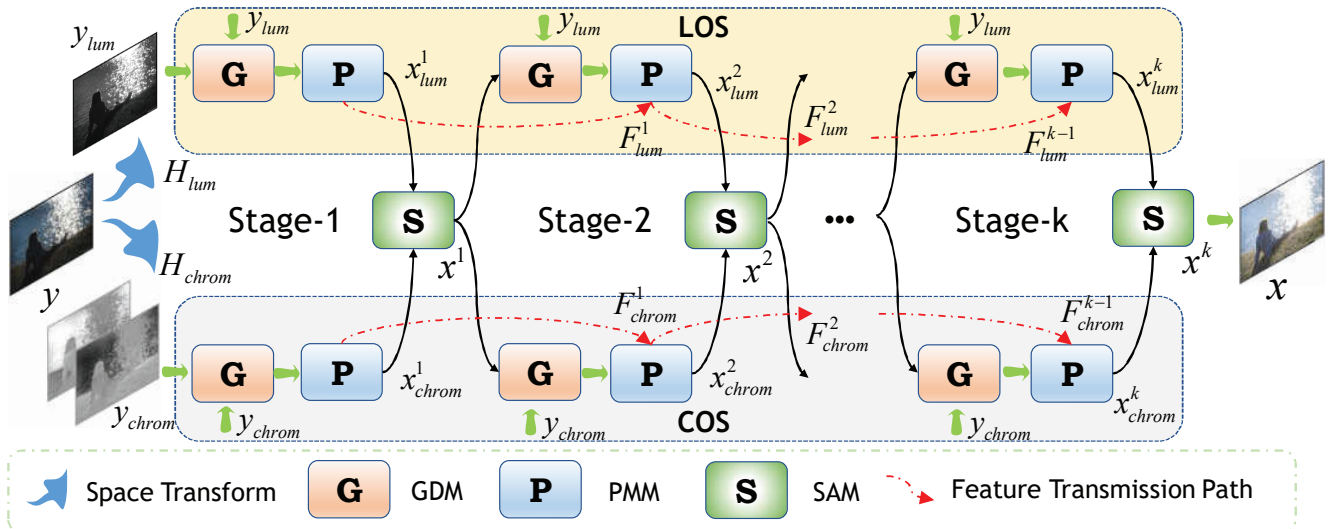


Fig. 1. The architecture of our DASUNet. The low-light image y is transformed to luminance space y_{lum} and chrominance space y_{chrom} . Then, they are respectively fed into luminance optimization stream (LOS) and chrominance optimization stream (COS). After k stages, the enhanced image x is produced.

of dual degradation model, which inherits the physical deterioration principle and interpretability. Further, an alternating optimization solution is designed to solve the proposed dual degradation model. Then, the iterative optimization rule is unfolded into a deep model, composing DASUNet, which enjoys the strengths of both the physical model and the deep network. Specifically, we propose a prior modeling module (PMM), combining the advantages of convolutions and Transformer [40]–[43], to learn more robust degradation-related priors from local and non-local region, which is used as the basic unit of DASUNet. Besides, we design a space aggregation module (SAM) to yield the clear images, which combines the reciprocity of dual degradation priors. We perform extensive experiments on several datasets to analyze and validate the effectiveness and superiority of our proposed DASUNet compared to other state-of-the-art methods.

In a nutshell, the main contributions of this work are summarized as follows:

- We propose a dual degradation model based on degradation specificity of low-light images on different spaces. It is unfolded to form dual degradation-inspired deep unfolding network for low-light image enhancement, which can jointly learn two degradation priors from luminance space and chrominance space. More importantly, dual degradation model empowers DASUNet with explicit physical insight, which improves the interpretability of enhancement model.
- We design a prior modeling module to obtain degradation-aware priors leveraging the local and long-range correlation extracted by convolution and Transformer. Moreover, a space aggregation module is proposed to interact two degradation models to yield vivid enhanced images.
- Extensive experiments conducted on multiple popular datasets show our proposed DASUNet outperforms other comparable low-light image enhancement methods.

The remainder of this paper is ordered as follows. In Section II, We briefly review the related works on low-light image enhancement and deep unfolding method. Section III introduces our proposed DASUNet. Experimental setting and extensive results are presented in Section IV. Finally, the proposed DASUNet are concluded in Section V.

II. RELATED WORK

In this section, we briefly survey the research progress on low-light image enhancement from traditional enhancement model and deep enhancement model. Moreover, deep unfolding method for image restoration is reviewed.

A. Low-light image enhancement

In the past years, low-light image enhancement has attracted increasing interesting and achieved remarkable advance. Generally speaking, low-light image enhancement can be classified into traditional enhancement method and deep enhancement method. Traditional enhancement model generally depends upon Retinex theory, which decomposes a low-light image to a luminance map and a reflectance map. Early enhancement methods achieved the image decomposition based on Gaussian filter [12], [13] or bright-pass filter [15]. However, the above methods could not obtain desired enhancement. Variational model [16] was also an alternative manner to address the log domain deviation. From then on, many researchers reformulated Retinex decomposition as an optimization task, which imposed many hand-crafted priors, such as noise prior [17], low-rank constraint [18], structure prior [19], [20], to constrain the solution space.

Recently, deep low-light image models have highly outperformed the traditional enhancement models not only in performance but also in running time. As a pioneering work, LLNet [21] lightened low-light images using the denoising auto-encoder. AGLNet [22] and DRBN [23] integrated multi-scale feature bands to enhance low-light images. To seek

higher performance, various Transformer frameworks [27], [28], [44], invertible network [45], and normalizing flow [29] were embedded into enhancement models. DCCNet [46] explored the color consistency of low-light images via a color histogram. UHDFour [47] found that luminance and noise can be separated in Fourier domain at low-light scenes. CSRNet [48] achieved the adjustable image enhancement via a conditional sequential modulation. DLN [49] proposed a back-projection module as the building block of enhancement network via exploring the correlation between darkening and lightening an image. MBPNet [25] combined multiple losses and a multi-scale network framework to progressively enhance the low-light images. Above methods generally learned the mapping relation between low-light images and normal-light images, but could not consider the physical imaging principle. Alternatively, some methods [31]–[33] attempted to decompose low-light images into reflectance and luminance maps via a data-driven deep model built on Retinex theory. Besides, more researchers [29], [30], [35], [50] have started to construct an unsupervised enhancement model to alleviate the shortage of paired images.

B. Deep unfolding method

Deep unfolding model inherits the advantages of the interpretability of physical models and the powerful representation capability of deep models driven by a large number of images, which has shown prominent performance in many vision tasks, e.g., super resolution [51]–[54] and compressive sensing [55]–[57]. Concretely speaking, deep unfolding model could optimize the iterative solver of physical models via some convolution networks in an end-to-end manner. For example, KXNet [51], DGUNet [56], and MADUN [58] unrolled proximal gradient descent into some specified network modules to tackle with the optimization problem of degradation models. USRNet [53], MDCUN [59], and DAUF [43] designed the half-quadratic splitting-based deep unfolding framework for the inverse problem in low-level vision. ADMM-CSNet [60] favored the merit of alternating direction method of multipliers to explore the application in deep end-to-end model. For low-light image enhancement, URetinex [36] proposed a Retinex theory-inspired unfolding model, however too many constraint terms hindered its performance. RUAS [35] and SCI [50] adopted a reference-free training mechanism to supervise the unfolding framework, limiting their performance. Unlike them, our method unfolds a novel dual degradation model based on space difference into an elaborated network, which learn two complementary and effective prior information to restore low-light images.

III. METHODOLOGY

In this section, we firstly introduce our designed dual degradation model (DDM) as the objective function. Then, an iterative optimization solution is designed as the solver of DDM. Moreover, we elaborate on dual degradation-inspired unfolding network (DASUNet) for low-light image enhancement, which is delineated on Figure 1. Finally, our loss function is described to end-to-end train our DASUNet.

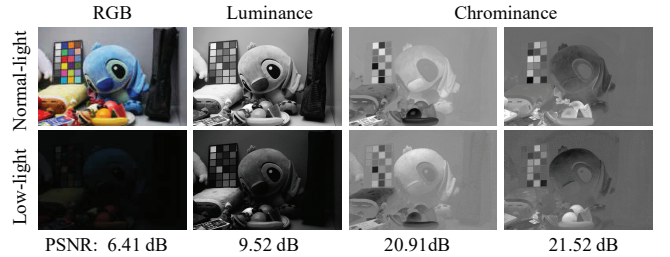


Fig. 2. The comparison of luminance and chrominance spaces. We can see that there are different distortion degrees in luminance and chrominance from quantitative and qualitative perspectives.

A. Dual Degradation Model

Fundamentally, given a low-light image $\mathbf{y} \in \mathbb{R}^{H \times W \times 3}$, this paper aims to recover a normal-light image $\mathbf{x} \in \mathbb{R}^{H \times W \times 3}$ from it. $H \times W \times 3$ denotes the spatial dimension of an image. The degradation model of low-light images can be described as:

$$\mathbf{y} = \mathbf{D}\mathbf{x} + \mathbf{n}, \quad (1)$$

where \mathbf{D} is a hybrid degradation operator, which may include luminance deterioration, color distortion, and detail loss [33], [61], and \mathbf{n} denotes the additive Gaussian white noise. Hence, we can recover \mathbf{x} by minimizing the following energy function:

$$\min_{\mathbf{x}} \frac{1}{2} \|\mathbf{y} - \mathbf{D}\mathbf{x}\|_2^2 + \lambda \mathcal{J}(\mathbf{x}), \quad (2)$$

where $\min_{\mathbf{x}} \frac{1}{2} \|\mathbf{y} - \mathbf{D}\mathbf{x}\|_2^2$ is the data fidelity term, $\mathcal{J}(\mathbf{x})$ represents the degradation prior term, and λ denotes the hyperparameter weighting the significance of prior term. Due to the ill-posedness of the degradation model, many hand-crafted prior items, e.g., non-local similarity [62], [63] and low-rank prior [64], are introduced to approximate a desired solution. However, above priors are hard to depict the universal structure of natural images. Recently, deep denoising prior [65], [66] is proposed to characterize the image-generic skeleton in a data-driven manner, which shows more competitive performance in many low-level vision tasks. Hence, this paper also adopts deep prior as the regularization constraint.

Traditional degradation models [62], [64] generally conduct in a single image space, e.g., RGB or Y, which could show single deterioration type. However, low-light images manifest diverse deterioration types, leading to less effectiveness of the above degradation models for their enhancements. Of note, we find the degradation specificity between luminance and chrominance spaces in low-light images [37]–[39], which is demonstrated in Figure 2. Literature [37] has analyzed the phenomenon from transformation matrix and demonstrated that chrominance map focuses more on structural and textural changes and illuminance map pays exclusive attention to brightness changes. One can see obvious degradation difference in luminance and chrominance spaces from Figure 2, which inspires us to design DDM to describe different deterioration process. DDM can be obtained via transforming Equation (2):

$$\min_{\mathbf{x}_{lum}, \mathbf{x}_{chrom}} \frac{1}{2} \|\mathbf{y}_{lum} - \mathbf{D}_{lum}\mathbf{x}_{lum}\|_2^2 + \lambda_1 \mathcal{J}(\mathbf{x}_{lum}) + \frac{1}{2} \|\mathbf{y}_{chrom} - \mathbf{D}_{chrom}\mathbf{x}_{chrom}\|_2^2 + \lambda_2 \mathcal{J}(\mathbf{x}_{chrom}) \quad (3)$$

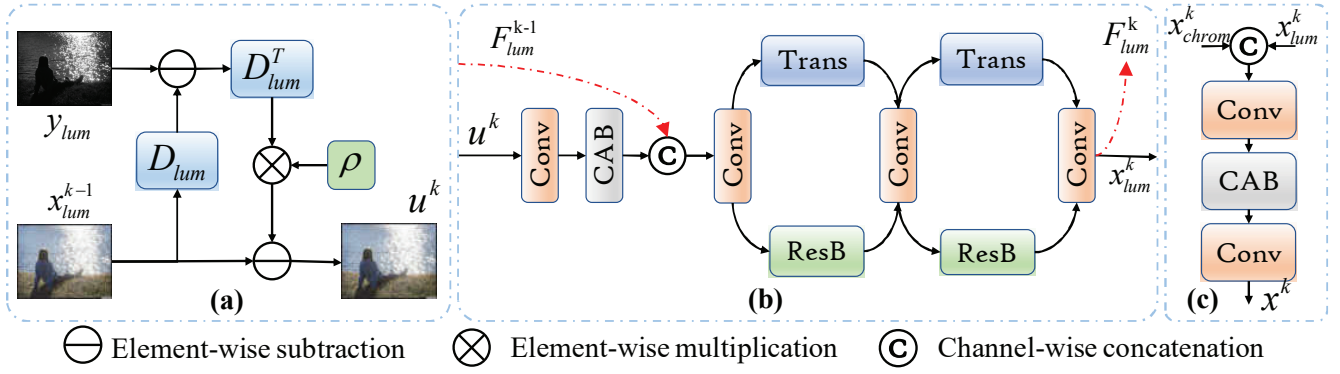


Fig. 3. The illustration of network structure of each phase. (a) Gradient Descent Module (GDM); (b) Prior Modelling Module (PMM); (c) Space Aggregation Module (SAM).

where \mathbf{D}_{lum} and \mathbf{D}_{chrom} refer to luminance and chrominance degradation operators, $\mathbf{x}_{lum} \in \mathbb{R}^{H \times W \times 1}$ and $\mathbf{y}_{lum} \in \mathbb{R}^{H \times W \times 1}$ denote luminance components of normal-light and low-light images, $\mathbf{x}_{chrom} \in \mathbb{R}^{H \times W \times 2}$ and $\mathbf{y}_{chrom} \in \mathbb{R}^{H \times W \times 2}$ denote chrominance components of normal-light and low-light images, $\mathcal{J}(\mathbf{x}_{lum})$ and $\mathcal{J}(\mathbf{x}_{chrom})$ denote the luminance space prior and chrominance space prior, λ_1 and λ_2 are two weighting parameters. More specifically, \mathbf{x}_{lum} , \mathbf{y}_{lum} , \mathbf{x}_{chrom} , and \mathbf{y}_{chrom} can be obtained via:

$$\begin{aligned} \mathbf{x}_{lum}, \mathbf{y}_{lum} &= \mathbf{H}_{lum}(\mathbf{x}, \mathbf{y}), \\ \mathbf{x}_{chrom}, \mathbf{y}_{chrom} &= \mathbf{H}_{chrom}(\mathbf{x}, \mathbf{y}), \end{aligned} \quad (4)$$

where \mathbf{H}_{lum} and \mathbf{H}_{chrom} signify the luminance and chrominance transform. For compactness, we omit the transformation processing in the following. Moreover, we can easily transform luminance and chrominance components to original RGB space via the inverse transformation of \mathbf{H}_{lum} and \mathbf{H}_{chrom} . DDM disentangles the intricate low-light degradation process into two easy independent degradation operators, which significantly reduce the modeling difficulty of the prior term.

B. Optimization Solution

To achieve accurate normal-light images from low-light images, we design an alternate optimization solution to solve DDM. Firstly, we separate Equation (3) into two independent objects to facilitate the optimization solution:

$$\min_{\mathbf{x}_{lum}} \frac{1}{2} \|\mathbf{y}_{lum} - \mathbf{D}_{lum} \mathbf{x}_{lum}\|_2^2 + \lambda_1 \mathcal{J}(\mathbf{x}_{lum}), \quad (5)$$

$$\min_{\mathbf{x}_{chrom}} \frac{1}{2} \|\mathbf{y}_{chrom} - \mathbf{D}_{chrom} \mathbf{x}_{chrom}\|_2^2 + \lambda_2 \mathcal{J}(\mathbf{x}_{chrom}), \quad (6)$$

where Equation (5) represents luminance degradation model and Equation (6) refers to chrominance degradation model. They can be parallelly updated in luminance and chrominance spaces.

Taking Equation (5) as example, it can be solved via proximal gradient algorithm [55], [56], which has been demonstrated its effectiveness in many inverse problems. Specifically, we can alternatively deduce the following updating rule to obtain an approximate solution:

$$u^k = \mathbf{x}_{lum}^{k-1} - \rho^k \mathbf{D}_{lum}^T (\mathbf{D}_{lum} \mathbf{x}_{lum}^{k-1} - \mathbf{y}_{lum}), \quad (7a)$$

$$\mathbf{x}_{lum}^k = Prox_{\lambda_1}(u^k), \quad (7b)$$

where \mathbf{x}_{lum}^k is the k -th updating solution, ρ^k denotes the updating stepsize, \mathbf{D}_{lum}^T is the transpose of \mathbf{D}_{lum} , $Prox_{\lambda_1}$ represents the proximal operator. Generally, the first item is called as the gradient descent and the second item is thought as the proximal mapping.

Similarly, chrominance degradation model is also solved by:

$$v^k = \mathbf{x}_{chrom}^{k-1} - \eta^k \mathbf{D}_{chrom}^T (\mathbf{D}_{chrom} \mathbf{x}_{chrom}^{k-1} - \mathbf{y}_{chrom}), \quad (8a)$$

$$\mathbf{x}_{chrom}^k = Prox_{\lambda_2}(v^k). \quad (8b)$$

Finally, we can obtain the output results during k -th updating process via:

$$\mathbf{x}^k = [\mathbf{H}_{lum}^T(\mathbf{x}_{lum}^k); \mathbf{H}_{chrom}^T(\mathbf{x}_{chrom}^k)], \quad (9)$$

where $\mathbf{H}_{lum}^T(\cdot)$ and $\mathbf{H}_{chrom}^T(\cdot)$ are the inverse transformation of luminance and chrominance transform. $[\cdot; \cdot]$ represents the space merging operation.

Based on above designed iteration optimization solution, we unfold each iterative step into corresponding modules to construct our DASUNet, which is shown in Figure 1. Specifically, our DASUNet is composed of k stages, each of which contains two parts, luminance optimization stream (LOS) and chrominance optimization stream (COS). Furthermore, we design a space aggregation module (SAM) to combine the output of each stage of COS and LOS, which can interact the complementary features learned from luminance and chrominance spaces to produce more high-quality normal-light restored images.

Luminance Optimization Stream. LOS is composed of gradient descent modules (GDM) and prior modeling modules (PMM), which are unfolded from Equation (7). Taking k -th stage for example, GDM adopts low-light luminance component \mathbf{y}_{lum} and the $(k-1)$ -th restored result \mathbf{x}_{lum}^{k-1} as inputs, which is depicted in Figure 3 (a). A non-trivial problem is the construction of the degradation operator \mathbf{D}_{lum} and its transpose \mathbf{D}_{lum}^T . Inspired by [55], [56], we employ a residual convolution block to simulate \mathbf{D}_{lum} and \mathbf{D}_{lum}^T . Their structure all adopt Conv-PReLU-Conv, and the channel numbers of two Convs are set to n and 1. For ρ^{k-1} , it is a learnable parameter that is updated in each epoch and initialized to 0.5.

Another important module is PMM, which is also thought as a denoising network in many works [65], [66]. Previous

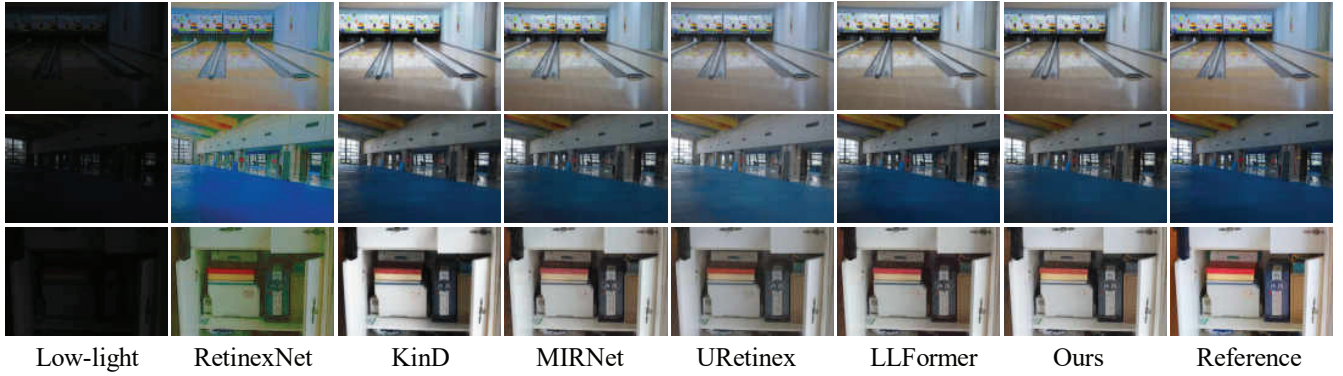


Fig. 4. The visual comparison on LOL dataset.

methods usually exploit convolution block, e.g., U-net and Resblock, to learn a universal image prior driven by tremendous specified-type images. However, they only extract local image prior via stacking more convolutions but cannot learn more representative long-range image structure. Recently, Transformer has been demonstrated its superiority for long-range information modeling in many vision tasks [40]–[43]. Motivated by them, we design a novel PMM, combining the strengths of convolution and Transformer, to model local and long-range structural knowledge, as shown in Figure 3(b). Moreover, some researchers [58], [59] found the information flow among adjacent stages limits the performance of deep unfolding networks and propose a memory-augmented mechanism to facilitate the information flow across stages. Consequently, we build a high-way feature transmission path among adjacent stages without any convolution to aggravate the model efficiency, as shown in Figure 1.

Specifically, the input is first fed into a convolution with kernel size of 3 and a channel attention block (CAB) [67] to extract shallow features. Then, two 3×3 convolutions with n channels are used to aggregate the shallow features and high-way features from previous stage. Next, the combined features are equally split into two parts from the channel dimension. One part is passed into a Resblock to learn local degradation prior and another part is inputted into a Transformer block to extract long-range degradation knowledge. Following that, an 1×1 convolution is used to combine them. To boost the interaction of local and long-range information, we conduct above Res-Trans operation again. Finally, the learned features are sent into high-way features transmission path to flow into the next stage and SAM to produce the restored results of this stage. Overall, LOS can be described as:

$$u^k = \text{GDM}_{\lambda_1}(\mathbf{x}_{lum}^k, \mathbf{x}_{lum}^{k-1}), \quad (10a)$$

$$\mathbf{x}_{lum}^k, \mathbf{F}_{lum}^k = \text{PMM}_{\lambda_1}(u^k, \mathbf{F}_{lum}^{k-1}). \quad (10b)$$

Chrominance Optimization Stream. COS has the same structure with LOS. Similarly, it is represented as:

$$v^k = \text{GDM}_{\lambda_2}(\mathbf{x}_{chrom}^k, \mathbf{x}_{chrom}^{k-1}), \quad (11a)$$

$$\mathbf{x}_{chrom}^k, \mathbf{F}_{chrom}^k = \text{PMM}_{\lambda_2}(v^k, \mathbf{F}_{chrom}^{k-1}). \quad (11b)$$

Space Aggregation Module. SAM is proposed to combine luminance prior and chrominance prior based on Equation (9).

It takes the outputs of LOS and COS as input to produce the enhanced normal-light image. Specifically, it firstly concatenate \mathbf{x}_{lum}^k and \mathbf{x}_{chrom}^k . Then, a 3×3 convolution with n channels is used to combine them. After that, a CAB is added to emphasize the significant features. Finally, we yield the enhanced images in this stage via a 3×3 convolution with 3 channels. SAM is shown in Figure 3(c) and can be written as below:

$$\mathbf{x}^k = \text{SAM}(\mathbf{x}_{lum}^k, \mathbf{x}_{chrom}^k). \quad (12)$$

In short, we summarized the optimization process of our proposed DASUNet in **Algorithm 1**.

Algorithm 1 The optimization process of our proposed DASUNet.

Input : Low-light image \mathbf{y} , Stage k

Output : Normal-light image \mathbf{x}

Initialization: $\mathbf{x}^0 = \mathbf{y}, \lambda, \eta$

for $t = 1, 2, \dots, k$ **do**

$$\begin{aligned}
 & \mathbf{x}_{lum}^t, \mathbf{y}_{lum}^t = \mathbf{H}_{lum}(\mathbf{x}^{t-1}, \mathbf{y}); \\
 & \mathbf{x}_{chrom}^t, \mathbf{y}_{chrom}^t = \mathbf{H}_{chrom}(\mathbf{x}^{t-1}, \mathbf{y}); \\
 & u^t = \text{GDM}_{\lambda_1}(\mathbf{y}_{lum}^t, \mathbf{x}_{lum}^{t-1}); \\
 & \mathbf{x}_{lum}^t, \mathbf{F}_{lum}^t = \text{PMM}_{\lambda_1}(u^t, \mathbf{F}_{lum}^{t-1}); \\
 & v^t = \text{GDM}_{\lambda_2}(\mathbf{y}_{chrom}^t, \mathbf{x}_{chrom}^{t-1}); \\
 & \mathbf{x}_{chrom}^t, \mathbf{F}_{chrom}^t = \text{PMM}_{\lambda_2}(v^t, \mathbf{F}_{chrom}^{t-1}); \\
 & \mathbf{x}^t = \text{SAM}(\mathbf{x}_{lum}^t, \mathbf{x}_{chrom}^t);
 \end{aligned}$$

C. Loss Function

Given N pairs of low/normal-light images $\{\mathbf{y}_i, \tilde{\mathbf{x}}_i\}, i = [1, 2, \dots, N]$, we can train our proposed DASUNet via the following loss function:

$$\mathcal{L} = \frac{1}{N} \sum_{i=1}^N \sum_{j=1}^k w^j \mathbb{C}(\mathbf{x}_i^j, \tilde{\mathbf{x}}_i), \quad (13)$$

where k is the stage number, w^j is the weighting parameter of the j -th stage, $\mathbb{C}(\cdot, \cdot)$ indicates the Charbonnier loss, and \mathbf{x}_i^j denotes the enhanced image of j -th stage of DASUNet. In our training, we set $w^k = 1$ and other $w^j = 0.1$.

Charbonnier loss is defined as below:

$$\mathbb{C}(x_1, x_2) = \sqrt{\|x_1 - x_2\|^2 + \epsilon^2}, \quad (14)$$

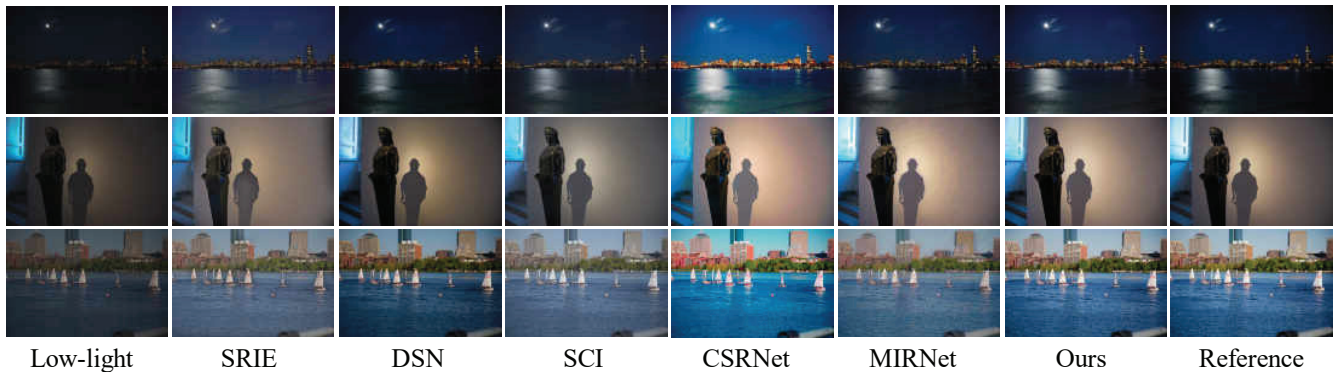


Fig. 5. The visual comparison on MIT-Adobe FiveK dataset.



Fig. 6. Visual comparisons on LOL-V2 dataset.

TABLE I

THE COMPARISON RESULTS OF OURS WITH OTHER STATE-OF-THE-ART METHODS ON LOL DATASET. BLOD INDICATES THE BEST RESULTS AND UNDERLINE MARKS THE SECOND-BEST RESULTS.

Methods	AGCWD	SRIE	LIME	ROPE	Zero-DCE	RetinexNet	En-GAN	KinD
PSNR	13.05	11.86	16.76	15.02	14.86	16.77	17.48	20.38
SSIM	0.4038	0.4979	0.5644	0.5092	0.5849	0.5594	0.6578	0.8045
LPIPS	0.4816	0.3401	0.3945	0.4713	0.3352	0.4739	0.3223	0.1593
Methods	KinD++	MIRNet	URetinex	Bread	DCCNet	LL-Former	UHDFour	Ours
PSNR	21.80	<u>24.14</u>	21.33	22.96	22.98	23.65	23.10	24.48
SSIM	<u>0.8316</u>	0.8302	0.7906	0.8121	0.7909	0.8102	0.8208	0.8455
LPIPS	<u>0.1584</u>	0.1311	0.1210	0.1597	0.1427	0.1692	0.1466	<u>0.1271</u>

where ϵ is a tiny positive number and is set to 1×10^{-3} in our all experiments.

IV. EXPERIMENTS AND RESULTS

A. Training Detail

Our DASUNet is conducted in PyTorch platform with an RTX 3090 GPU. The channel number n for all module (without clear statement) is set to 64 and the stage number k is initialized as 4 in our experiments. Adam optimizer with default setting ($\beta_1 = 0.9$ and $\beta_2 = 0.99$) is used as the training solver of DASUNet. The initial learning rate is specified as 2×10^{-4} and gradually decreases to 1×10^{-6} during 500 epochs via the cosine annealing strategy. Moreover, we also use the warming up strategy (3 epochs) to steady the training of our DASUNet. Training samples are randomly cropped

with size of 256×256 and then rotated and flipped for data augmentation. For convenience, images are firstly transformed to YCbCr space for training or inference and are finally re-transformed back to RGB domain for impartial evaluation.

B. Benchmark and Evaluation Index

We evaluate the effectiveness of our DASUNet on five popular benchmarks: LOL dataset [31], MIT-Adobe FiveK dataset [68], LOL-V2 dataset [23], MEF dataset [69], and DICM dataset [70]. LOL dataset is comprised of 500 paired of low/normal-light images, in which 485 pairs are used for training and the rest is used for test. MIT-Adobe FiveK dataset contains 5000 low-light images from various real scenes. Like other methods, we use the images retouched by expert-C as reference images. The first 4500 pairs images are set as the

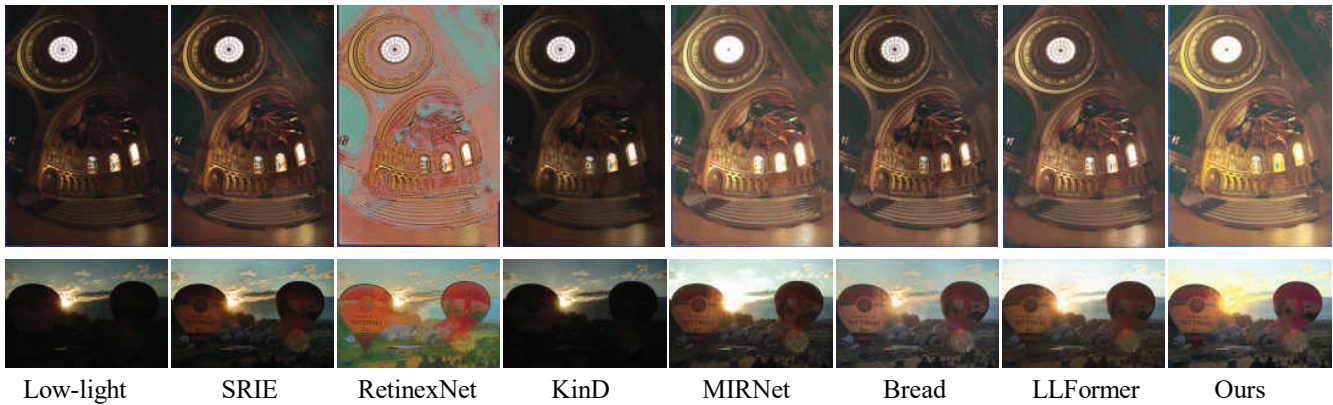


Fig. 7. Visual comparisons on MEF dataset.

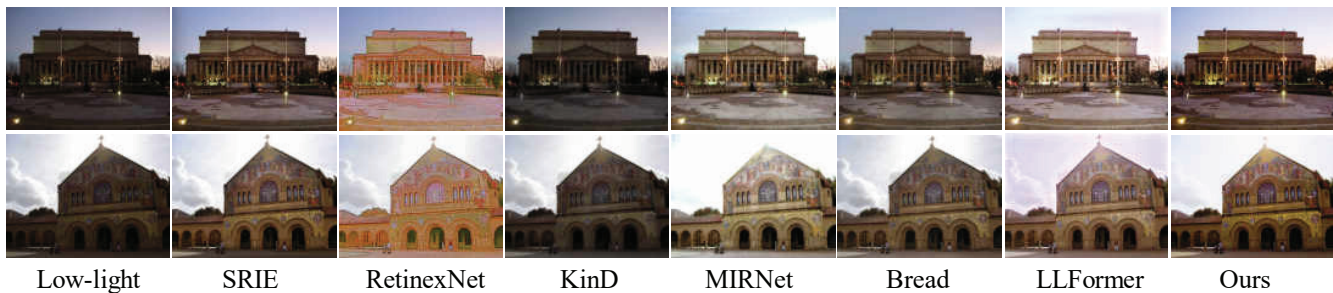


Fig. 8. Visual comparisons on DICM dataset.

TABLE II

THE COMPARISON RESULTS OF OURS WITH OTHER STATE-OF-THE-ART METHODS ON MIT-ADOBE FIVEK DATASET. BLOD INDICATES THE BEST RESULTS AND UNDERLINE MARKS THE SECOND-BEST RESULTS.

Methods	SRIE	LIME	IAT	DSN	DSL	SCI	CSRNet	MIRNet	Ours
PSNR	18.44	13.28	18.08	19.58	20.26	20.73	20.93	<u>23.78</u>	25.54
SSIM	0.7905	0.7276	0.7888	0.8308	0.8150	0.7816	0.7875	<u>0.8995</u>	0.9244
LPIPS	0.1467	0.1573	0.1364	0.0874	0.1759	0.1066	0.1297	<u>0.0714</u>	0.0477

TABLE III

THE COMPARISON RESULTS OF OURS WITH OTHER STATE-OF-THE-ART METHODS ON LOL-V2 DATASET. BLOD INDICATES THE BEST RESULTS AND UNDERLINE MARKS THE SECOND-BEST RESULTS.

Methods	SRIE	LIME	En-GAN	Zero-DCE	URetinex	SNRANet	UHDFour	Ours
PSNR	14.45	15.24	18.64	18.06	19.78	21.41	<u>21.78</u>	22.11
SSIM	0.5240	0.4151	0.6767	0.5795	0.8427	0.8475	0.8542	<u>0.8512</u>

training set and the last 500 pairs images are selected as test set. LOL-V2 dataset contains 789 pairs of normal/low-light images, in which 689 pairs are used to train the enhancement model and 100 pairs are used as testset. MEF and DICM are two unpaired datasets without reference images. They are respectively composed of 17 and 69 images, which usually are used to evaluate the generalization ability of enhancement algorithms. Three full-reference evaluators, PSNR, SSIM, and LPIPS [71], are selected as objective metrics for LOL, MIT-Adobe FiveK, and LOL-V2 datasets with reference images. For unpaired datasets, we introduce a no-reference evaluator NIQE [72] to assess their performance.

C. Comparison with State-of-the-Art Methods

To evaluate the performance of our proposed DASUNet, we compare our results with fifteen classical low-light image enhancement methods which include four traditional models (AGCWD [73], SRIE [16], LIME [14], and ROPE [74]), two unsupervised methods (Zero-DCE [30] and EnlightenGAN [29]), five recent deep black-box methods (MIRNet [75], Bread [39], LL-Former [28], and UHDFour [47]), and four deep Retinex-based methods (RetinexNet [31], KinD [32], KinD++ [76], and URetinex [36]), on LOL dataset. Quantitative comparison results are summarized in Table I. It can easily observe that our method outperforms other comparison



Fig. 9. The visual comparison of different degradation models.

TABLE IV
THE COMPARISON RESULTS OF OURS WITH OTHER STATE-OF-THE-ART METHODS ON MEF AND DICM DATASETS IN TERMS OF NIQE.

Datasets	SRIE	Zero-DCE	RetinexNet	KinD	MIRNet	Bread	LLFormer	Ours
MEF	3.2041	3.3088	4.9043	3.5598	3.1915	3.5677	3.2847	3.0813
DICM	3.3657	3.0973	4.3143	3.5135	3.1533	3.4063	3.5154	2.9475

TABLE V
THE COMPARISON RESULTS OF DIFFERENT DEGRADATION MODELS ON LOL DATASET.

Methods	Single model	Single model	Double model	Triple model	Triple model
Space	RGB	YCbCr	Y-CbCr	R-G-B	Y-Cb-Cr
PSNR \uparrow	23.43	23.25	24.48	22.22	23.60
SSIM \uparrow	0.8281	0.8285	0.8455	0.8248	0.8317
LPIPS \downarrow	0.1498	0.1433	0.1271	0.1600	0.1446
Time (s)	0.27	0.27	0.38	0.49	0.49

methods in PSNR and SSIM and achieves the second-best results in LPIPS evaluator. Qualitative results are presented in Figure 4. As can be seen, RetinexNet cannot achieve expected enhancement images and KinD produces over-smoothing restored images. URetinex shows the color deviation on the ground. MIRNet and LLFormer seem to be under-enhanced and noisy. However, the enhanced result by our DASUNet shows more vivid details and more natural scene light, which remove some artifacts and noise that cannot be eliminated by other methods.

Moreover, we conduct experiments on MIT-Adobe FiveK dataset to demonstrate the generalization capability of our proposed DASUNet. We compare our model with eight state-of-the-art methods including SRIE [16], LIME [14], IAT [44], SCI [50], DSN [45], DSLR [77], CSRNet [48], and MIRNet [75] in Table II. As tabulated in Table II, our method significantly surpasses the second-best methods, MIRNet, in terms of PSNR, SSIM, and LPIPS. To show the effectiveness of our DASUNet, visual comparisons are manifested in Figure 5. One can observe that SRIE and DSN cannot achieve favorable enhancements. CSRNet overenhances the low-light images. MIRNet encounters ring artifacts in the second row of image. Overall, our DASUNet produces impressive enhanced images.

We compare our results with seven methods, including SRIE [16], LIME [14], EnlightenGAN [29], Zero-DCE [30], URetinex [36], SNRANet [27], and UHDFour [47], on LOL-V2 dataset. As shown in Table III, we outperform other comparison methods in PSNR and achieve the second-best performance in SSIM. Visual comparisons are shown in Figure 6. As shown in Figure 6, LIME and URetinex over-enhance the low-light images. Zero-DCE produces under-enhanced results.

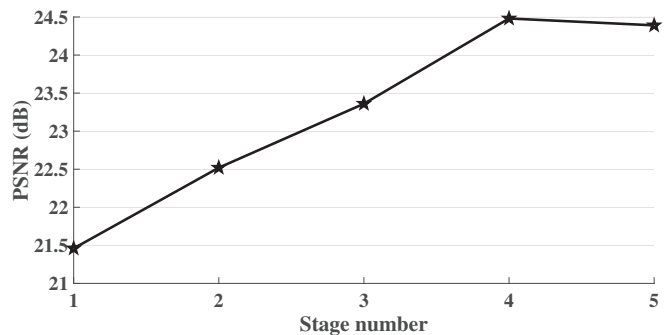


Fig. 10. Ablation study of stage number

UHDFour encounters the color cast in the first-line image. Our method yields visual-pleased results.

Besides, we compare our results with SRIE [16], Zero-DCE [30], RetinexNet [31], KinD [32], MIRNet [75], Bread [39], and LLFormer [28] on MEF and DICM datasets. As shown in Table IV, we obtain the best performance on two datasets in terms of NIQE. Visual comparisons are shown in Figure 7 and 8. RetinexNet produces unnatural looks, and KinD achieves under-enhanced results. While MIRNet over-enhances low-light images. LLFormer produces checkboard artifacts which only uses transformer to model long-range information but ignores local details. It can be observed that our method produces impressive enhancement images.

D. Ablation study

Dual degradation model. Based on the degradation specificity between luminance and chrominance spaces, we proposed a DDM for low-light image enhancement. To demon-

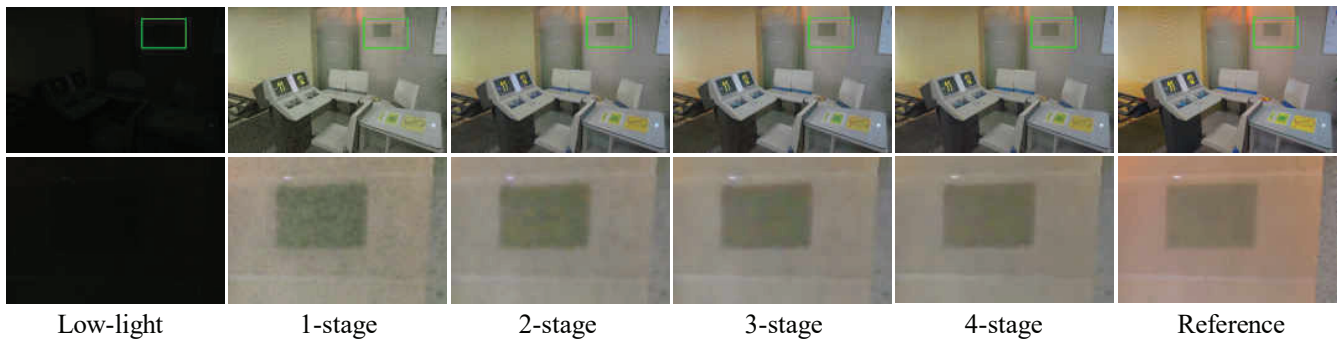


Fig. 11. The visual comparison of different stages.

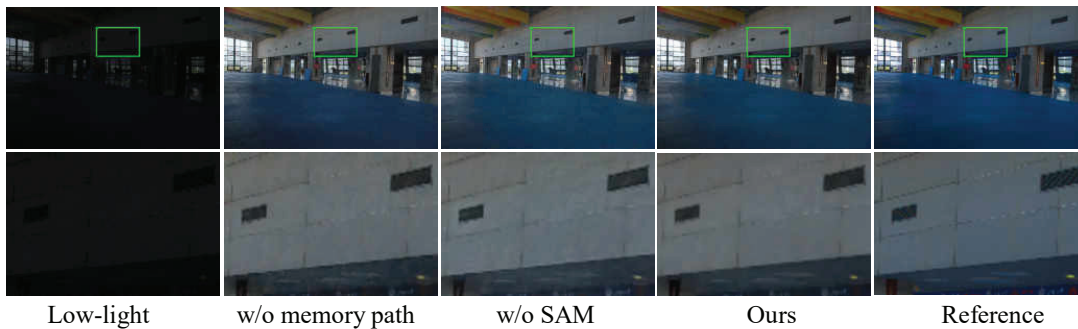


Fig. 12. Visual comparisons of memory path and SAM.

TABLE VI
THE ABLATION STUDY OF UNFOLDING FRAMEWORK ON LOL DATASET.

Resblock	Transformer	Number	PSNR \uparrow	SSIM \uparrow	LPIPS \downarrow	Time (s)
✓		2	22.88	0.8161	0.1712	0.23
	✓	2	23.42	0.8299	0.1452	0.43
✓	✓	1	23.38	0.8262	0.1537	0.32
✓	✓	2	24.48	0.8455	0.1271	0.38
✓	✓	3	23.64	0.8326	0.1374	0.45

TABLE VII
THE ABLATION STUDY OF FEATURE PATH AND SAM ON LOL DATASET.

SAM	feature path	PSNR \uparrow	SSIM \uparrow	LPIPS \downarrow	Time (s)
✓		22.08	0.8034	0.1829	0.37
	✓	22.00	0.8239	0.1572	0.38
✓	✓	24.48	0.8455	0.1271	0.38

strate its effectiveness, we conduct some comparison experiments on various color spaces and degradation models on LOL dataset, the results of which are presented in Table V. Single model and triple model denotes one degradation model and three degradation models on corresponding spaces. One can see from Table V that the design philosophy behind DDM is effective. Single model cannot consider the the degradation specificity on different spaces and triple model could lose the mutual benefits between homogeneous degradation spaces. Visual comparison of different degradation models are illustrated in Figure 9. Single model introduces some visual artifacts and triple model yields some blurs, while our model produce clearer result.

Stage number. It is well-known that the stage number k is essential for iteration optimization solution. We explore the performance difference of different stage numbers and experimental results are delineated in Figure 10. When k exceeds 4, the enhancement performance cannot be further improved. Consequently, the stage number in our experiments is set to 4. Visual comparison are shown in Figure 11. One can see clearer results with stage advancement.

Unfolding framework. In PMM, we model local and long-range prior information leveraging Resblock and Transformer. To analyze their effects, we perform a set of ablation experiments via breaking them down. As listed in Table VI, the performance will be decreased by 1.60dB and 1.06 dB when deleting Resblock and Transformer. Furthermore, we investigate the effect of the number of Resblock and Transformer. It can obtain the best performance when the number is 2 as shown in Table VI, which can boost the interaction between local and long-range information. More interactions could hinder the long-distance flow of information.

Besides, we study the effect of SAM and high-way feature path. As shown in Table VII, the performance will be heavily

TABLE VIII
THE INVESTIGATION OF PMM ON LOL DATASET.

Model	PSNR \uparrow	SSIM \uparrow	LPIPS \downarrow
a	21.89	0.7659	0.2193
b	22.96	0.8203	0.1672
c	23.51	0.8317	0.1417
d (Ours)	24.48	0.8455	0.1271

decreased when deleting SAM and high-way feature path. It demonstrates the importance of SAM and high-way feature path for space prior combination and feature flow. Visual comparisons are shown in Figure 12.

E. Investigation on PMM

Considering the degradation specificity between luminance and chrominance spaces of low-light images, we propose DASUNet to learn two different priors from luminance and chrominance components. In this subsection, we will investigate whether we need to design different building blocks for PMM in two different optimization flows. As shown in Figure 2, luminance component has more severe distortion while chrominance components show slight degradation in quality. It is intuitive that we seem to design complicated module for LOS and less complex module for COS. To obtain a clear answer, we construct four models by using convolution and transformer to make a comparison on LOL dataset. In model a, we use classical Resblock as the building block of PMM. In model b, LOS uses Resblock and COS exploits Resblock-Transformer module. The configuration of model c is the opposite of that of model b. Two optimization flows of Model d all use Resblock-Transformer module to learn extract prior information, namely DASUNet. Experimental results are presented in Table VIII. One can observe that model a obtains the worse results due to the limited prior representation ability of PMM. When we use Resblock-Transformer to replace Resblock in model b and c, the performance will be improved by more than 1dB in PSNR. It indicates more powerful module in PMM can extract more robust features to improve the enhancement performance. Model c produces better quantitative indexes than model b, which seems to be consistent with the above intuition. However, it can yield best results when two optimization flows all use Resblock-Transformer with powerful representation capability. Actually, the ability of any deep modules stem from training data. In other words, two identical network blocks can learn different priors from different training samples. Hence, we use more powerful building block in two optimization flows to construct our DASUNet, which can yield more impressive enhancement performance.

F. Running Time

We report the average running time of our method and recent proposed deep learning-based methods on LOL dataset in Figure 13. Also, we list model parameters of all test methods in Figure 13. Although LLFormer and MIRNet can achieve noticeable performance, they are heavy in model size. URtinetex and Zero-DCE show compact model design, but their

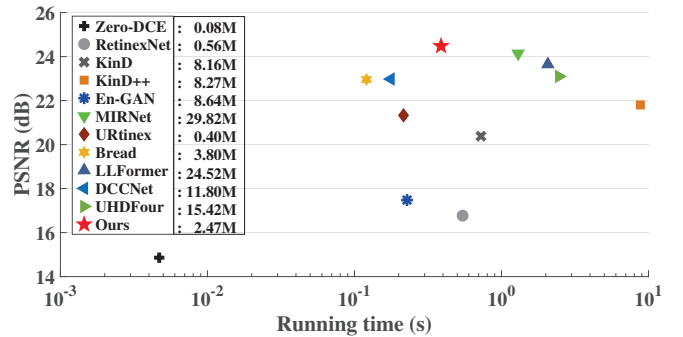


Fig. 13. The comparison on running time and parameters.

performance is poorer than ours. One can see that our method achieves the best performance with an acceptable running time and a relatively economic model size. It embodies a favorable trade-off between the effectiveness and efficiency of our proposed model.

V. CONCLUSION

In this paper, we have proposed a dual degradation-inspired deep unfolding method (DASUNet) for low-light image enhancement. Specifically, we design a dual degradation model (DDM) based on the degradation specificity among luminance and chrominance spaces. An alternative optimization solution is proposed to solve it and is unfolded into specified network modules to construct our DASUNet, which contains a new prior modeling module (PMM) to capture the local and long-range information and a space aggregation module (SAM) to combine dual degradation priors. Extensive experimental results on five benchmark datasets validate the superiority of our DASUNet for low-light image enhancement. In future, we will explore more low-level vision tasks based on DDM.

REFERENCES

- [1] Z. Cui, G. Qi, L. Gu, S. You, Z. Zhang, and T. Harada, "Multitask AET with orthogonal tangent regularity for dark object detection," in *Proceedings of the IEEE International Conference on Computer Vision*, 2021, pp. 2533–2542. 1
- [2] T. Ma, L. Ma, X. Fan, Z. Luo, and R. Liu, "PIA: parallel architecture with illumination allocator for joint enhancement and detection in low-light," in *Proceedings of the ACM International Conference on Multimedia*. ACM, 2022, pp. 2070–2078. 1
- [3] Y. Sasagawa and H. Nagahara, "YOLO in the dark - domain adaptation method for merging multiple models," in *Proceedings of the European Conference on Computer Vision*, vol. 12366, 2020, pp. 345–359. 1
- [4] T. Wang, T. Zhang, K. Zhang, H. Wang, M. Li, and J. Lu, "Context attention fusion network for crowd counting," *Knowl. Based Syst.*, vol. 271, p. 110541, 2023. 1
- [5] J. Ye, C. Fu, G. Zheng, D. P. Paudel, and G. Chen, "Unsupervised domain adaptation for nighttime aerial tracking," in *Proceedings of the IEEE Conference on Computer Vision and Pattern Recognition*, 2022, pp. 8886–8895. 1
- [6] J. Ye, C. Fu, G. Zheng, Z. Cao, and B. Li, "Darklighter: Light up the darkness for UAV tracking," in *IEEE/RSS International Conference on Intelligent Robots and Systems*, 2021, pp. 3079–3085. 1
- [7] S. Hira, R. Das, A. Modi, and D. Pakhomov, "Delta sampling R-BERT for limited data and low-light action recognition," in *IEEE Conference on Computer Vision and Pattern Recognition Workshops*, 2021, pp. 853–862. 1
- [8] C. M. Nguyen, E. R. Chan, A. W. Bergman, and G. Wetzstein, "Diffusion in the dark: A diffusion model for low-light text recognition," *CoRR*, vol. abs/2303.04291, 2023. 1

- [9] C. Sakaridis, D. Dai, and L. V. Gool, "ACDC: the adverse conditions dataset with correspondences for semantic driving scene understanding," in *Proceedings of the IEEE International Conference on Computer Vision*, 2021, pp. 10745–10755. **1**
- [10] H. Gao, J. Guo, G. Wang, and Q. Zhang, "Cross-domain correlation distillation for unsupervised domain adaptation in nighttime semantic segmentation," in *Proceedings of the IEEE Conference on Computer Vision and Pattern Recognition*, 2022, pp. 9903–9913. **1**
- [11] Y. Liao, J. Xie, and A. Geiger, "KITTI-360: A novel dataset and benchmarks for urban scene understanding in 2d and 3d," *IEEE Trans. Pattern Anal. Mach. Intell.*, vol. 45, no. 3, pp. 3292–3310, 2023. **1**
- [12] D. J. Jobson, Z. Rahman, and G. A. Woodell, "Properties and performance of a center/surround retinex," *IEEE Trans. Image Process.*, vol. 6, no. 3, pp. 451–462, 1997. **1, 2**
- [13] —, "A multiscale retinex for bridging the gap between color images and the human observation of scenes," *IEEE Trans. Image Process.*, vol. 6, no. 7, pp. 965–976, 1997. **1, 2**
- [14] X. Guo, Y. Li, and H. Ling, "LIME: low-light image enhancement via illumination map estimation," *IEEE Trans. Image Process.*, vol. 26, no. 2, pp. 982–993, 2017. **1, 7, 8**
- [15] S. Wang, J. Zheng, H. Hu, and B. Li, "Naturalness preserved enhancement algorithm for non-uniform illumination images," *IEEE Trans. Image Process.*, vol. 22, no. 9, pp. 3538–3548, 2013. **1, 2**
- [16] X. Fu, D. Zeng, Y. Huang, X. S. Zhang, and X. Ding, "A weighted variational model for simultaneous reflectance and illumination estimation," in *Proceedings of the IEEE Conference on Computer Vision and Pattern Recognition*, 2016, pp. 2782–2790. **1, 2, 7, 8**
- [17] M. Li, J. Liu, W. Yang, X. Sun, and Z. Guo, "Structure-revealing low-light image enhancement via robust retinex model," *IEEE Trans. Image Process.*, vol. 27, no. 6, pp. 2828–2841, 2018. **1, 2**
- [18] X. Ren, W. Yang, W. Cheng, and J. Liu, "LR3M: robust low-light enhancement via low-rank regularized retinex model," *IEEE Trans. Image Process.*, vol. 29, pp. 5862–5876, 2020. **1, 2**
- [19] J. Xu, Y. Hou, D. Ren, L. Liu, F. Zhu, M. Yu, H. Wang, and L. Shao, "STAR: A structure and texture aware retinex model," *IEEE Trans. Image Process.*, vol. 29, pp. 5022–5037, 2020. **1, 2**
- [20] B. Cai, X. Xu, K. Guo, K. Jia, B. Hu, and D. Tao, "A joint intrinsic-extrinsic prior model for retinex," in *Proceedings of the IEEE International Conference on Computer Vision*, 2017, pp. 4020–4029. **1, 2**
- [21] K. G. Lore, A. Akintayo, and S. Sarkar, "Llnet: A deep autoencoder approach to natural low-light image enhancement," *Pattern Recognit.*, vol. 61, pp. 650–662, 2017. **1, 2**
- [22] F. Lv, Y. Li, and F. Lu, "Attention guided low-light image enhancement with a large scale low-light simulation dataset," *Int. J. Comput. Vis.*, vol. 129, no. 7, pp. 2175–2193, 2021. **1, 2**
- [23] W. Yang, S. Wang, Y. Fang, Y. Wang, and J. Liu, "From fidelity to perceptual quality: A semi-supervised approach for low-light image enhancement," in *Proceedings of the IEEE Conference on Computer Vision and Pattern Recognition*, 2020, pp. 3060–3069. **1, 2, 6**
- [24] H. Wang, Z. Li, and X. Hou, "Versatile denoising-based approximate message passing for compressive sensing," *IEEE Trans. Image Process.*, vol. 32, pp. 2761–2775, 2023. **1**
- [25] K. Zhang, C. Yuan, J. Li, X. Gao, and M. Li, "Multi-branch and progressive network for low-light image enhancement," *IEEE Trans. Image Process.*, vol. 32, pp. 2295–2308, 2023. **1, 3**
- [26] Y. Wang, R. Wan, W. Yang, H. Li, L. Chau, and A. C. Kot, "Low-light image enhancement with normalizing flow," in *Proceedings of the AAAI Conference on Artificial Intelligence*, 2022, pp. 2604–2612. **1**
- [27] X. Xu, R. Wang, C. Fu, and J. Jia, "Snr-aware low-light image enhancement," in *Proceedings of the IEEE Conference on Computer Vision and Pattern Recognition*, 2022, pp. 17693–17703. **1, 3, 8**
- [28] T. Wang, K. Zhang, T. Shen, W. Luo, B. Stenger, and T. Lu, "Ultra-high-definition low-light image enhancement: A benchmark and transformer-based method," in *Proceedings of the AAAI Conference on Artificial Intelligence*, 2023, pp. 1–10. **1, 3, 7, 8**
- [29] Y. Jiang, X. Gong, D. Liu, Y. Cheng, C. Fang, X. Shen, J. Yang, P. Zhou, and Z. Wang, "Enlightengan: Deep light enhancement without paired supervision," *IEEE Trans. Image Process.*, vol. 30, pp. 2340–2349, 2021. **1, 3, 7, 8**
- [30] C. Guo, C. Li, J. Guo, C. C. Loy, J. Hou, S. Kwong, and R. Cong, "Zero-reference deep curve estimation for low-light image enhancement," in *Proceedings of the IEEE Conference on Computer Vision and Pattern Recognition*, 2020, pp. 1777–1786. **1, 3, 7, 8**
- [31] C. Wei, W. Wang, W. Yang, and J. Liu, "Deep retinex decomposition for low-light enhancement," in *British Machine Vision Conference*, 2018, p. 155. **1, 3, 6, 7, 8**
- [32] Y. Zhang, J. Zhang, and X. Guo, "Kindling the darkness: A practical low-light image enhancer," in *Proceedings of the ACM International Conference on Multimedia*, 2019, pp. 1632–1640. **1, 3, 7, 8**
- [33] R. Wang, Q. Zhang, C. Fu, X. Shen, W. Zheng, and J. Jia, "Underexposed photo enhancement using deep illumination estimation," in *Proceedings of the IEEE Conference on Computer Vision and Pattern Recognition*, 2019, pp. 6849–6857. **1, 3**
- [34] M. Fan, W. Wang, W. Yang, and J. Liu, "Integrating semantic segmentation and retinex model for low-light image enhancement," in *Proceedings of the ACM International Conference on Multimedia*, 2020, pp. 2317–2325. **1**
- [35] R. Liu, L. Ma, J. Zhang, X. Fan, and Z. Luo, "Retinex-inspired unrolling with cooperative prior architecture search for low-light image enhancement," in *Proceedings of the IEEE Conference on Computer Vision and Pattern Recognition*, 2021, pp. 10561–10570. **1, 3**
- [36] W. Wu, J. Weng, P. Zhang, X. Wang, W. Yang, and J. Jiang, "Uretinex-net: Retinex-based deep unfolding network for low-light image enhancement," in *Proceedings of the IEEE Conference on Computer Vision and Pattern Recognition*, 2022, pp. 5891–5900. **1, 3, 7, 8**
- [37] H. Wang, X. Yan, X. Hou, J. Li, Y. Dun, and K. Zhang, "Division gets better: Learning brightness-aware and detail-sensitive representations for low-light image enhancement," *CoRR*, vol. abs/2307.09104, 2023. **1, 3**
- [38] Y. Atoum, M. Ye, L. Ren, Y. Tai, and X. Liu, "Color-wise attention network for low-light image enhancement," in *Proceedings of the IEEE Conference on Computer Vision and Pattern Recognition*, 2020, pp. 2130–2139. **1, 3**
- [39] X. Guo and Q. Hu, "Low-light image enhancement via breaking down the darkness," *Int. J. Comput. Vis.*, vol. 131, no. 1, pp. 48–66, 2023. **1, 3, 7, 8**
- [40] A. Dosovitskiy, L. Beyer, A. Kolesnikov, D. Weissenborn, X. Zhai, T. Unterthiner, M. Dehghani, M. Minderer, G. Heigold, S. Gelly, J. Uszkoreit, and N. Houlsby, "An image is worth 16x16 words: Transformers for image recognition at scale," in *International Conference on Learning Representations*, 2021. **2, 5**
- [41] Z. Liu, Y. Lin, Y. Cao, H. Hu, Y. Wei, Z. Zhang, S. Lin, and B. Guo, "Swin transformer: Hierarchical vision transformer using shifted windows," in *Proceedings of the IEEE International Conference on Computer Vision*, 2021, pp. 9992–10002. **2, 5**
- [42] K. Zhang, Y. Li, J. Liang, J. Cao, Y. Zhang, H. Tang, R. Timofte, and L. V. Gool, "Practical blind denoising via swin-conv-unet and data synthesis," *CoRR*, vol. abs/2203.13278, 2022. **2, 5**
- [43] Y. Cai, J. Lin, H. Wang, X. Yuan, H. Ding, Y. Zhang, R. Timofte, and L. V. Gool, "Degradation-aware unfolding half-shuffle transformer for spectral compressive imaging," in *Advances in Neural Information Processing Systems*, 2022. **2, 3, 5**
- [44] Z. Cui, K. Li, L. Gu, S. Su, P. Gao, Z. Jiang, Y. Qiao, and T. Harada, "You only need 90k parameters to adapt light: a light weight transformer for image enhancement and exposure correction," in *British Machine Vision Conference*, 2022, p. 238. **3, 8**
- [45] L. Zhao, S. Lu, T. Chen, Z. Yang, and A. Shamir, "Deep symmetric network for underexposed image enhancement with recurrent attentional learning," in *Proceedings of the IEEE International Conference on Computer Vision*, 2021, pp. 12055–12064. **3, 8**
- [46] Z. Zhang, H. Zheng, R. Hong, M. Xu, S. Yan, and M. Wang, "Deep color consistent network for low-light image enhancement," in *Proceedings of the IEEE Conference on Computer Vision and Pattern Recognition*, 2022, pp. 1889–1898. **3**
- [47] C. Li, C. Guo, M. Zhou, Z. Liang, S. Zhou, R. Feng, and C. C. Loy, "Embedding fourier for ultra-high-definition low-light image enhancement," in *International Conference on Learning Representations*, 2023. **3, 7, 8**
- [48] J. He, Y. Liu, Y. Qiao, and C. Dong, "Conditional sequential modulation for efficient global image retouching," in *Proceedings of European Conference Computer Vision*, vol. 12358, 2020, pp. 679–695. **3, 8**
- [49] L. Wang, Z. Liu, W. Siu, and D. P. Lun, "Lightening network for low-light image enhancement," *IEEE Trans. Image Process.*, vol. 29, pp. 7984–7996, 2020. **3**
- [50] L. Ma, T. Ma, R. Liu, X. Fan, and Z. Luo, "Toward fast, flexible, and robust low-light image enhancement," in *Proceedings of the IEEE Conference on Computer Vision and Pattern Recognition*, 2022, pp. 5627–5636. **3, 8**
- [51] J. Fu, H. Wang, Q. Xie, Q. Zhao, D. Meng, and Z. Xu, "Kxnet: A model-driven deep neural network for blind super-resolution," in *Proceedings of European Conference Computer Vision*, vol. 13679, 2022, pp. 235–253. **3**

- [52] Z. Luo, Y. Huang, S. Li, L. Wang, and T. Tan, "Unfolding the alternating optimization for blind super resolution," in *Advances in Neural Information Processing Systems*, 2020. 3
- [53] K. Zhang, L. V. Gool, and R. Timofte, "Deep unfolding network for image super-resolution," in *Proceedings of the IEEE Conference on Computer Vision and Pattern Recognition*, 2020, pp. 3214–3223. 3
- [54] W. Dong, C. Zhou, F. Wu, J. Wu, G. Shi, and X. Li, "Model-guided deep hyperspectral image super-resolution," *IEEE Trans. Image Process.*, vol. 30, pp. 5754–5768, 2021. 3
- [55] W. Chen, C. Yang, and X. Yang, "FSOINET: feature-space optimization-inspired network for image compressive sensing," in *IEEE International Conference on Acoustics, Speech and Signal Processing*, 2022, pp. 2460–2464. 3, 4
- [56] C. Mou, Q. Wang, and J. Zhang, "Deep generalized unfolding networks for image restoration," in *Proceedings of the IEEE Conference on Computer Vision and Pattern Recognition*, 2022, pp. 17378–17389. 3, 4
- [57] H. Wang, Z. Li, and X. Hou, "Versatile denoising-based approximate message passing for compressive sensing," *IEEE Trans. Image Process.*, vol. 32, pp. 1–15, 2023. 3
- [58] J. Song, B. Chen, and J. Zhang, "Memory-augmented deep unfolding network for compressive sensing," in *Proceedings of the ACM International Conference on Multimedia*, 2021, pp. 4249–4258. 3, 5
- [59] G. Yang, M. Zhou, K. Yan, A. Liu, X. Fu, and F. Wang, "Memory-augmented deep conditional unfolding network for pansharpening," in *Proceedings of the IEEE Conference on Computer Vision and Pattern Recognition*, 2022, pp. 1778–1787. 3, 5
- [60] Y. Yang, J. Sun, H. Li, and Z. Xu, "Admm-csnet: A deep learning approach for image compressive sensing," *IEEE Trans. Pattern Anal. Mach. Intell.*, vol. 42, no. 3, pp. 521–538, 2020. 3
- [61] C. Zheng, D. Shi, and W. Shi, "Adaptive unfolding total variation network for low-light image enhancement," in *Proceedings of the International Conference on Computer Vision*, 2021, pp. 4419–4428. 3
- [62] K. Zhang, X. Gao, D. Tao, and X. Li, "Single image super-resolution with non-local means and steering kernel regression," *IEEE Trans. Image Process.*, vol. 21, no. 11, pp. 4544–4556, 2012. 3
- [63] K. Zhang, D. Tao, X. Gao, X. Li, and Z. Xiong, "Learning multiple linear mappings for efficient single image super-resolution," *IEEE Trans. Image Process.*, vol. 24, no. 3, pp. 846–861, 2015. 3
- [64] W. Dong, G. Shi, and X. Li, "Nonlocal image restoration with bilateral variance estimation: A low-rank approach," *IEEE Trans. Image Process.*, vol. 22, no. 2, pp. 700–711, 2013. 3
- [65] W. Dong, P. Wang, W. Yin, G. Shi, F. Wu, and X. Lu, "Denoising prior driven deep neural network for image restoration," *IEEE Trans. Pattern Anal. Mach. Intell.*, vol. 41, no. 10, pp. 2305–2318, 2019. 3, 4
- [66] K. Zhang, Y. Li, W. Zuo, L. Zhang, L. V. Gool, and R. Timofte, "Plug-and-play image restoration with deep denoiser prior," *IEEE Trans. Pattern Anal. Mach. Intell.*, vol. 44, no. 10, pp. 6360–6376, 2022. 3, 4
- [67] Y. Zhang, K. Li, K. Li, L. Wang, B. Zhong, and Y. Fu, "Image super-resolution using very deep residual channel attention networks," in *Proceedings of European Conference Computer Vision*, vol. 11211, 2018, pp. 294–310. 5
- [68] V. Bychkovsky, S. Paris, E. Chan, and F. Durand, "Learning photographic global tonal adjustment with a database of input / output image pairs," in *Proceedings of the IEEE Conference on Computer Vision and Pattern Recognition*, 2011, pp. 97–104. 6
- [69] K. Ma, K. Zeng, and Z. Wang, "Perceptual quality assessment for multi-exposure image fusion," *IEEE Trans. Image Process.*, vol. 24, no. 11, pp. 3345–3356, 2015. 6
- [70] C. Lee, C. Lee, and C. Kim, "Contrast enhancement based on layered difference representation of 2d histograms," *IEEE Trans. Image Process.*, vol. 22, no. 12, pp. 5372–5384, 2013. 6
- [71] R. Zhang, P. Isola, A. A. Efros, E. Shechtman, and O. Wang, "The unreasonable effectiveness of deep features as a perceptual metric," in *Proceedings of the IEEE Conference on Computer Vision and Pattern Recognition*, 2018, pp. 586–595. 7
- [72] A. Mittal, A. K. Moorthy, and A. C. Bovik, "No-reference image quality assessment in the spatial domain," *IEEE Trans. Image Process.*, vol. 21, no. 12, pp. 4695–4708, 2012. 7
- [73] S. Huang, F. Cheng, and Y. Chiu, "Efficient contrast enhancement using adaptive gamma correction with weighting distribution," *IEEE Trans. Image Process.*, vol. 22, no. 3, pp. 1032–1041, 2013. 7
- [74] X. Wu, Y. Sun, A. Kimura, and K. Kashino, "Reflectance-oriented probabilistic equalization for image enhancement," in *IEEE International Conference on Acoustics, Speech and Signal Processing*, 2021, pp. 1835–1839. 7
- [75] S. W. Zamir, A. Arora, S. H. Khan, M. Hayat, F. S. Khan, M. Yang, and L. Shao, "Learning enriched features for real image restoration and enhancement," in *Proceedings of European Conference Computer Vision*, vol. 12370, 2020, pp. 492–511. 7, 8
- [76] Y. Zhang, X. Guo, J. Ma, W. Liu, and J. Zhang, "Beyond brightening low-light images," *Int. J. Comput. Vis.*, vol. 129, no. 4, pp. 1013–1037, 2021. 7
- [77] S. Lim and W. Kim, "DSLR: deep stacked laplacian restorer for low-light image enhancement," *IEEE Trans. Multim.*, vol. 23, pp. 4272–4284, 2021. 8